

Experimental study on pore pressure generation mode of saturated remolded loess during dynamic liquefaction

Jianmin Liu^{1,2}, Tingting Guo^{1,2,a}, Guangcheng Zhang^{1,2} and Haiqing Fu^{1,2}

1Shandong Institute of Earthquake Engineering, Jinan 250021, China

2Earthquake Administration of Shandong Province, Jinan 250014, China

a)Corresponding author: gtt.yy@163.com

Abstract.Through dynamic triaxial tests of the saturated remolded loess, the pore water pressure generation characteristics of the samples are analysed during liquefaction processes. Based on dynamic triaxial test results, pore pressure generation characteristics of remolded sample are discussed, the effect of confining pressure on the generation of excess pore water pressure is evaluated, the particularity of pore pressure generation by comparing with the predecessor's research results is pointed out and the normalized pore pressure growth model is given. Finally, fitting curve of pore water pressure growth is drawn by using this model and fitting parameters are given.

1. Introduction

Nowadays, our country is still in seismic active period and the loess area is located in strong earthquake activity area [1]. In this area, the seismic disasters such as land slide and subsidence often occur during earthquakes. Under earthquake loads, pore water pressure can increase rapidly and effective stress can decrease, which will lead to soil liquefaction [2]. Therefore, it is important to research pore pressure generation and seismic stability during liquefaction of loess area. Initial liquefaction and cyclic mobility both can cause extensive damage during earthquakes, including sand boils, settlement and tilting of buildings and bridge abutments, collapse of offshore structures, lateral spreading and cracking of slopes, flow failures of earth dams, cracking of pavements, and flotation to the ground surface of buried concrete tanks.

Cyclic loading of saturated granular soils can result in the generation of excess pore water pressure under undrained conditions. In loose soils, the developed excess pore water pressure can be as high as the existing overburdened pressure on soil. This condition corresponds to zero effective stress and is called initial liquefaction of the granular soil [3]. Fitting pore pressure formula is given combining with the influence of dynamic size, dynamic form, vibration frequency and consolidation ratio to saturated loess vibration of pore pressure [4]. Pore pressure growth model of saturated undisturbed loess under dynamic loading is given [5-6].

For pore pressure change regular pattern of saturated undisturbed loess specimen under dynamic loading, many pore pressure growth models have been given, but research result about remolded sample is little. In this paper, loess liquefaction is studied experimentally with a dynamic triaxial apparatus. Through the vibration liquefaction test of saturated remolded loess, the pore pressure generation characteristics of remolded sample is discussed, the particularity of pore pressure generation by comparing with the predecessor's research, is pointed out, and the normalized pore pressure growth model is given finally.



The samples used in the experiment are all prepared by dry pack compaction methods which are determined by averagedry density of soil sample in situ test. Samplesize are50 * 100 mm and samples are compacted for five layers; Samples are prepared by special compaction instrument and each layer needs contact well to avoid stratified phenomenon.

3. The test method

After the completion of the samples preparation, put them in a cylinder for vacuum suction to attain saturation; Then make the samples saturated by back pressure on dynamic triaxial apparatus, and when pore water pressure coefficient is equal or greater than 0.98, drainage consolidation of samples can be done. After the completion of the consolidation,close drain valve and use different dynamic load in test. In FIGURE2, The test can recordthe dynamic loading, dynamic pore pressure and dynamic strain test data.

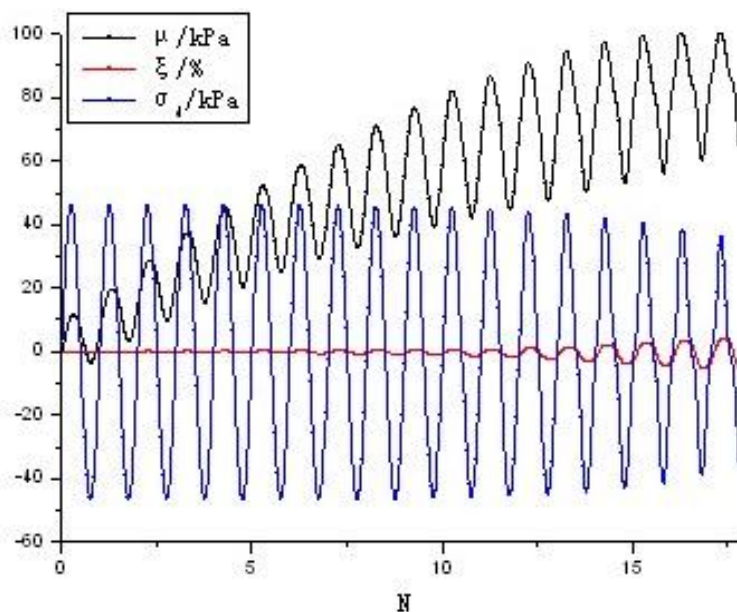


FIGURE2. Test record curve under dynamic loading

4. Analysis of test results

Through the analysis of pore pressure growth pattern by Jianmin Zhang, pore pressure growth curve is divided into A, B and C three categories (FIGURE3). It is used to simulate the seismic load which producethe pore pressure curve in the front, central and rear of seismic time history. Among them, type B curve area can better simulate hole pressure growth process of sand and loess soilpore water pressure growth curve is more close to type A curve area.

$$U_d = U_f (1 - e^{-\beta \frac{N}{N_f}}) \quad (1)$$

$$U_d = \frac{2}{\pi} U_f \sin^{-1} \left(\frac{N}{N_f} \right)^{\frac{1}{2\alpha}} \quad (2)$$

$$U_d = U_f \left[\frac{1}{2} \left(1 - \cos \pi \frac{N}{N_f} \right) \right]^b \quad (3)$$

(1) Type A pore water pressure growth curve

(2) Type B pore water pressure growth curve

(3) Type C pore water pressure growth curve

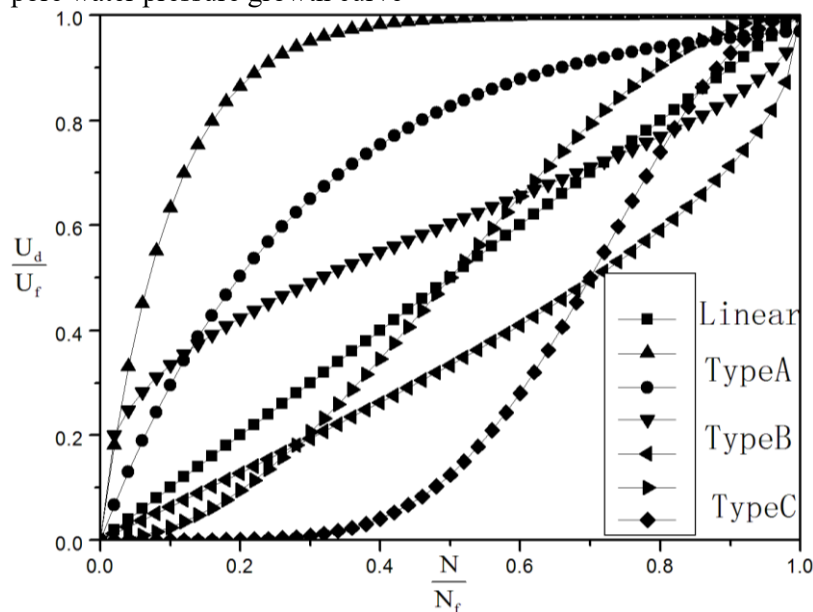


FIGURE3. Pore pressure growthRegional division

From pore water pressure growth curve under dynamic loading in figure 2, it can be seen that pore water pressure growth characteristics of remolded saturated loess sample is different from sand sample. This is mainly due to the unique structural characteristics and different content of clay in loess.

Figure 4 shows the results of the tests performed on specimens, that is, the excess pore water pressure (μ = measured excess pore water pressure) is presented versus the number of loading cycles (N), for shear stress levels of 25, 30, 35, 40 and 50 kPa. As can be seen from Figure 4, the excess pore water pressure increased significantly during the first 10 loading cycles for all shear stress levels, and continued its development at a slower rate with further application of loading cycles.

From figure 4, we also can see that the specimen tested at 25 kPa shear stress showed a progressive increase with increasing number of loading cycles. The excess pore water pressure ratio at this stress level was 3% after the first cycle, and ascended to approximately 38% at the end of 50 loading cycles. Similarly, at the biggest applied shear stress of 50 kPa, the excess pore water pressure ratio progressively increased from 10% at the end of the first cycle of loading to 100% after 17 loading cycles. At this point the specimen has reached full liquefaction in 17 cycles. It is clear that as the shear stress level increases, more excess pore water pressure is generated for the same number of loading cycles.

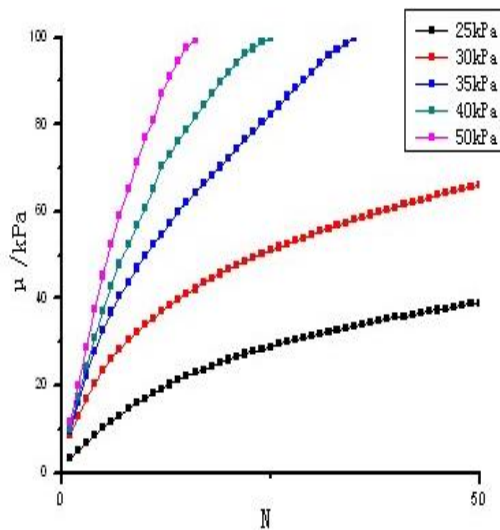


FIGURE 4. Excess pore water pressure generation as a function of number of loading cycles

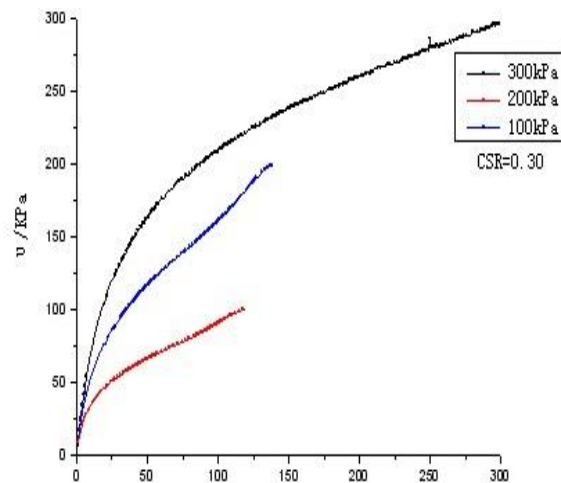


FIGURE 5. Comparison of excess pore

water pressure measurements from $\sigma_3=100\text{kPa}$, 200kPa and 300kPa specimens at $\text{CSR}=0.30$

Figure 5 displays the comparison at the smallest shear stress level of $\text{CSR}=0.30$. The shapes of the pore water pressure responses of the big and small confining pressure specimens are again similar. The main difference is that the excess pore water pressure in the big confining pressure is about 5% more than it in the small confining pressure. This difference appears to be maintained approximately constant at all loading cycles. Interestingly, the rate of excess pore water pressure generation are similar in the different confining pressure (FIGURE 6).

From figure 6, we can see that pore water pressure growth characteristics of saturated remolded loess samples are different from sand during vibration process. In the early vibration days, the pore pressure is growing faster, when the cycles ratio is 0.2, pore pressure ratio has risen to about 0.5; and with vibration continues, pore pressure ratio rising will slow down and reach the final stability, pore water pressure will present a fast-slow-flat trend. During the whole process, the change of pore water pressure will not appear sharply or sudden increase phenomenon, but gradually become stable. This regular pattern is different from saturated loose sand. Based on this, the author put forward pore water pressure growth normalized relations model of saturated reshaping loess samples as following:

$$\frac{U_d}{U_f} = \left(\frac{N}{N_f}\right)^\beta \sin\left[\frac{\pi}{2} \left(\frac{N}{N_f}\right)^\alpha\right]$$

Where U_f : maximum pore pressure under liquefaction, U_d : instantaneous pore pressure under vibration, N_f : liquefaction cyclic, N : vibration cyclic, β are parameters of test which are determined by dynamic load size, vibration frequency, α the nature of the earth soil such as mineral composition, grain size distribution and density; α is smaller, the curve shape is more fullness, α is 0.34 in this paper.

Using this model, the fitting curve of pore water pressure growth is shown in figure 7:

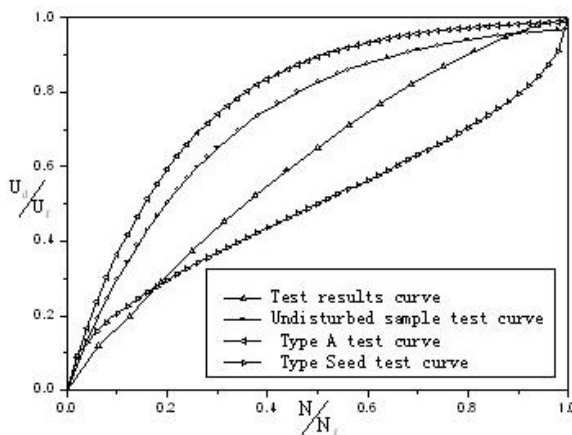


FIGURE 6. Different types of pore water pressure growth curve

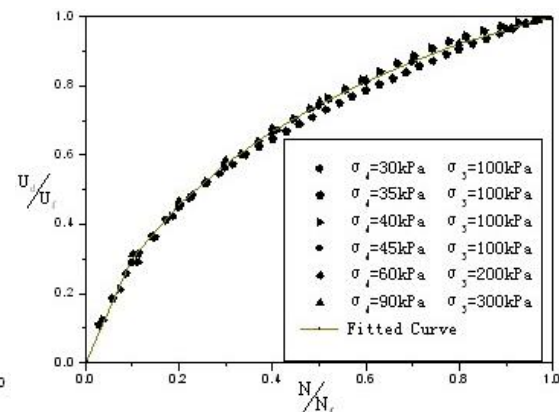


FIGURE 7. Fitting results of pore water pressure growth curve

5. Conclusion

The excess pore water pressure generation in saturated remolded loess is evaluated using stress-controlled and undrained cyclic triaxial tests. Then, the effect of confining pressure on the generation of excess pore water pressure is evaluated by comparing the responses of 100kPa, 200kPa and 300kPa. This comparison shows that, the excess pore water pressure generation in different confining pressure is similar in general. The pore water pressure growth characteristics of saturated remolded loess samples are different from sands'. Through the analysis of data, pore water pressure growth model is established.

Acknowledgments

[1] Liu Jian-min, Male, Master graduate student, Mainly engaged in the study of soil dynamics, tel: (15963101199).

[2] Shandong Provincial Natural Science Foundation, China (ZR2014DQ022)

Title: Research on Statistical Analysis and Numerical Simulation of "Avoiding Belt" Width of Active Fault

[3] Contractal Research Project of Earthquake Administration of Shandong Province, China (13Y86)

[4] Spark Program of Earthquake Sciences, China (XH16014)

References

- [1] Wang Lanmin 2003 *Loess Dynamics* (Beijing: Seismological Press) p282
- [2] Ishihara Ket al 1990 Liquefaction induced flow slide in the collapsible loess deposit in Soviet Tajik *Soils and Foundations*. 473-87
- [3] Seed HB 1979 Soil Liquefaction and Cyclic Mobility Evaluation for Level Ground During Earthquakes *Journal of the Geotechnical Engineering Division*. 2201-255
- [4] SUN Haimei, WANG Lanmin 2010 Experimental study of development of strain and pore water pressure during liquefaction of saturated Lanzhou loess *Rock and Soil Mechanics*. 113464-3468
- [5] SHE Yuexin, LIU Hanlong 2006 Study on pore water pressure mode and cyclic softening of saturated compacted loess *Northwestern Seismological Journal*. 2123-128
- [6] SHE Yuexin, LIU Hanong, Gao yufeng 2002 Study on liquefaction mechanism and pore water pressure mode of saturated original loess *Rock and Soil Mechanics* 4395-399
- [7] Castro, G, Liquefaction and Cyclic 1975 Mobility of Saturated Sands, *Journal of the Geotechnical Engineering Division*. 6551-569
- [8] Dobry, R 1985 Liquefaction of Soils During Earthquakes National Research Council (NRC) *Committee on Earthquake Engineering*. CETS-EE-001

- [9] Finn, W. D. L, Lee.K.Wand Martin. G. R1977 An Effective Stress Model for Liquefaction*Journal of the Geotechnical Engineering Division.*6517-533
- [10] Ishihara1996 *SoilBehaviour in Earthquake Geotechnics* (Oxford:Clarendon Press) p350-358